PREDICTING MICROSTRUCTURAL-LEVEL RESIDUAL STRESSES AND CRACK PATHS IN CERAMICS

V.R. VEDULA, S.J. GLASS, Sandia National Laboratories, Albuquerque, NM 87185
D.M. SAYLOR, G.S. ROHRER, Carnegie Mellon University, Pittsburgh, PA 15213
W.C. CARTER, Massachusetts Institute of Technology, Cambridge, MA 02139

Abstract

Microstructural-level residual stresses arise in ceramics due to thermal expansion anisotropy. The magnitude of these stresses can be very high and may cause spontaneous microcracking during the processing of these materials. The orientation data obtained by backscattered electron diffraction and grain boundary energies obtained by AFM were used in conjunction with an object oriented finite element analysis package (OOF) to predict the magnitude of residual stresses in alumina. Crack initiation and propagation were also simulated based on the Griffith fracture criterion.

Keywords: Ceramics, object oriented finite element analysis, residual stresses, crack paths

1. Introduction

Residual stresses arise in ceramics during processing as a result of thermal expansion anisotropy and crystallographic misorientation across the grain boundaries. In brittle materials, the thermal strains that result during cooling from the sintering temperature can be comparable to the fracture strain of the material leading to internal cracking known as "spontaneous microcracking". Residual stresses are also critical to the R-curve behavior that occurs in ceramics (Bennison and Lawn 1989).

Polycrystalline materials consist of many grains randomly oriented with respect to each other. Cubic crystals possess isotropic thermal expansion

DISCLAIMER

(α_{11}= α_{22}= α_{33}) in that spherical regions remain spherical after a temperature change, whereas in non-cubic systems, a sphere becomes an ellipsoid. Therefore, when a material with non-cubic crystal symmetry is subject to a temperature change, each grain will attempt to strain differently than its neighbors, resulting in residual stresses and strains in the material. The onset of microcracking depends on the grain (crystal) size and below a critical value, no spontaneous microcracking occurs (Green 1998). The stresses generated in a material do not depend on the grain size, however, the strain energy does. Assuming that enough stress and potential microcrack formation sites are available, it has been shown that the formation of microcracks in ceramics is governed by the energy criterion (Kuszyk and Bradt 1973).

This paper presents a novel methodology to predict residual stresses in materials using experimentally determined crystallographic orientations and grain boundary energies. Crystallographic orientations and relative grain boundary energies were obtained using electron backscattered patterns (EBSP) and atomic force microscopy (AFM) respectively. The critical temperature for microcrack formation in alumina was calculated as a function of grain size.

2. Experimental Details

The orientations of individual grains on the surface of a polycrystalline alumina (99.99%) sample were obtained using electron backscattered diffraction (EBSD) (OIM, TSL, Inc.). The final polishing step used colloidal silica and then the samples were thermally grooved at 1550°C for 100 hours. The width and depth of the thermal grooves formed by the grain boundaries were measured by atomic force microscopy (AFM) to determine the ratio of the grain boundary free energy to the surface free energy. The details of the measurements and the orientation and grain boundary energy data are presented in an accompanying paper (Glass et al. 1999). The orientations and grain boundary energies were used to predict the residual stresses in alumina using object oriented finite element analysis (OOF).

3. Finite Element Analysis

OOF is an object oriented finite element analysis software program developed at NIST (OOF 1999). It is designed to investigate the response of microstructures to mechanical and thermal loads. The program performs thermoelastic calculations in two dimensions (plane strain or plane stress) using 3-node triangular elements. A digital image of a microstructure, either from an optical/electron microscope or a result of a computer simulation can be used for analysis. The user specifies crystallographic orientations, elastic, and thermal properties for the various regions (grains) in the microstructure. Based on this information, a finite element grid with associated properties is generated on which mechanical and/or thermal loading can be applied. A solution is then obtained for the specified boundary conditions, distortion, and temperature change.

The elements are designed to fail under the Griffith criterion, which states that a crack will propagate when the total surface energy required to propagate the crack can be supplied by the elastic energy stored in the body;

$$2l\gamma < \frac{1}{2} \sigma \varepsilon dV \qquad (1)$$

where l is the crack length and γ is the surface energy of the cracked interface. The element size is used to specify the characteristic crack length and the volume of integration is the element area (per unit depth).

The analysis involves the following steps:

(a) Thermal and mechanical loads are applied and the microstructure is equilibrated to determine stress/strain distribution.
(b) The energy balance is computed.
(c) If an element reaches the critical energy density (i.e., favorable for cracking), the direction of the maximum principle stress is found. Assuming that the crack plane is perpendicular to the maximum principal stress, C_{11} is set to 0 and all other components of the stiffness matrix C_{ij} are multiplied by a factor of 0.5 (arbitrarily chosen). The elements thus reduce their moduli anisotropically to simulate a crack.
(d) The microstructure is re-equilibrated and the stress distribution is re-calculated.
(e) The procedure is repeated until no more elements mutate or one or more cracks become unstable causing fracture into two or more fragments.

4. Results and Discussion

The orientations of grains, surface energies of grains and grain boundaries, elastic, and thermal properties were input into OOF to predict the residual stresses. The orientations obtained by EBSD were input as a set of Euler angles (α, β, γ). The elastic stiffness and coefficients of thermal expansion for α-alumina (hexagonal crystal symmetry) used in the analysis were; C_{11}=466 GPa, C_{12}=127 GPa, C_{13}=117 GPa, C_{33}=506 GPa, C_{44}=235 GPa, α_{11}=8.6x10^{-6} /°C, and α_{33}=9.3x10^{-6} /°C. The energy required for crack propagation through a grain is $2\gamma_s$ and through a grain boundary is $2\gamma_{intergranular}=(2\gamma_s - \gamma_{gb})$, where γ_s is the surface energy of grains and γ_{gb} is the grain boundary energy. γ_{gb} values were obtained from AFM groove measurements. The surface energy of grains (γ_s) was taken as 2 J/m^2 and that of individual boundaries were calculated using $\gamma_{intergranular}=(4 - \gamma_{gb})/2$. $\gamma_{intergranular}$ varied between 0.59 and 1.17 J/m^2. The grain boundary elements were assigned the elastic properties of glass (isotropic crystal symmetry), E=70 GPa and ν=0.23. The elements in the model representing grains were assigned a surface energy of 2 J/m^2 and the boundary elements were assigned their respective γ_{GB} values. The number of elements was

25600. The calculations were performed under plane stress and free boundary conditions.

The properties of the grain boundary glass phase are expected to influence the stress distribution and critical temperature for microcracking. Two different glass compositions were considered for grain boundary phase, namely, a high CaO and a high MgO glass. A high CaO glass has $\alpha \approx 9.5 \times 10^{-6}$ /°C, which results in tensile residual stresses at grain boundaries, whereas for a high MgO glass ($\alpha \approx 5 \times 10^{-6}$ /°C), compressive stresses result at the grain boundaries (Powell-Dogan and Heuer 1990). These compositions and associated properties were chosen as they represent the bounds on the type of grain boundary glass phase typically found in alumina.

The alumina microstructure shown in Fig. 1(a) is used for analysis. The maximum principal stress σ_{11} for a temperature difference of -1160°C for high CaO grain boundary glass phase is shown in Fig. 1(b). The maximum and minimum stress regions (+369 and –128 MPa) are marked * and # respectively. As can be seen, very high stresses develop at the grain boundaries due to crystallographic misorientations in conjunction with thermal expansion anisotropy in alumina. The stresses were found to drop drastically away from the boundaries. The maximum stress is comparable to typical fracture strengths of this material. Internal stresses in alumina have been estimated at 100 and 155 MPa from spectroscopic measurements and theoretical calculations respectively (Bennison and Lawn 1989).

The effect of grain size on the critical temperature for microcracking in alumina was determined using the same microstructure by varying the width of the image, i.e, different length scales were used to represent different grain sizes. The expected inverse square root grain size relationship was found (Case et al. 1980), as shown in Fig. 2. The critical grain size for microcracking for an alumina sample cooled from a 1600°C sintering temperature with high CaO glass grain boundary phase was 179 μm and with high MgO phase was 71 μm. Experimentally, grain size values have been reported between 40-400 μm. It should be noted that plane stress conditions underestimate the residual stress values, hence in reality, the critical grain size values are expected to be lower.

Microcrack propagation was simulated using the procedure described above with increasing temperature difference. Fig. 1(c) shows initiation of microcracks at the triple junctions when ΔT=-1500°C. It has been shown numerically that the largest stress intensification occurs at the triple junctions (Evans 1978). With increasing temperature difference (thermal strain), microcracks initiated at new sites and coalescence of microcracks was also observed to form large cracks. At ΔT=-2000°C, out of 1212 grain boundary elements, 266 were cracked, shown in Fig. 1(d). As can be seen, damage occurred at several regions and some of the boundaries were completely cracked. It has been shown that the inverse square root relationship seen here for microcrack initiation holds for damage evolution with increasing misfit strain and it can be described by a three parameter Weibull distribution (Zimmerman et. al. 1999).

5. Conclusions

In brittle materials such as ceramics, cooling from the sintering temperature often creates sufficiently high stresses to cause internal microcracking. The magnitude of these stresses was predicted using an object oriented finite element analysis and experimentally determined orientations and grain boundary energies. In order to determine if there is a direct correlation between the boundaries that were cracked in OOF and misorientation across the boundaries, a large number of such calculations need to be performed and data compared with experimental observations of cracks. It is important to note that besides stresses, other factors that determine the onset of microcracking include the size and location of existing flaws as these can act as nucleation sites for microcracks.

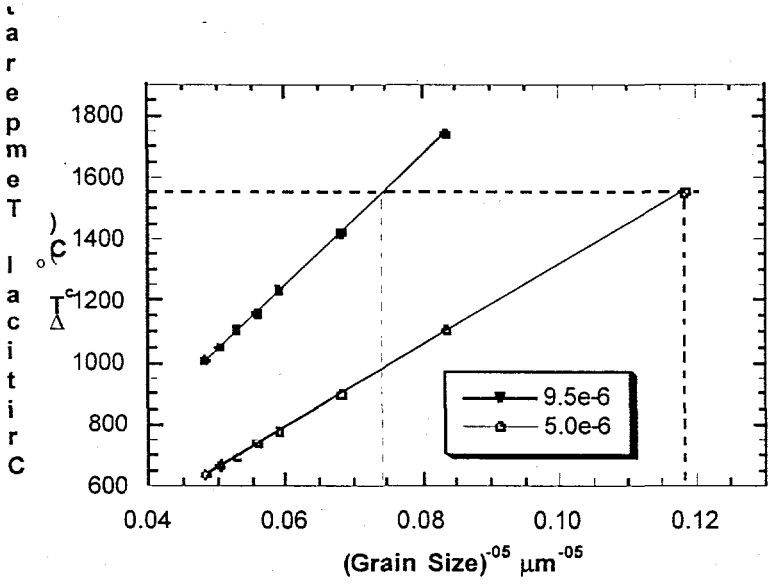

Fig. 2: Critical temperature difference vs. grain size in alumina for two different grain boundary properties (α=9.5x10^{-6} and 5x10^{-6} °/C)

References

Case, E.D., Smyth, J.R., and Hunter, O. (1980) Grain-size dependence of microcrack initiation in brittle materials, *Journal of Materials Science*, Vol. 15, pp. 149-53.

Evans, A.G. (1978) Microfracture from thermal expansion anisotropy – I. Single phase systems, *Acta Metallurgica*, Vol. 26, pp. 1845-53.

Glass, S.J., Vedula, V.R., Saylor, D.M., and Rohrer, G.S. (1999) Application of Electron backscattered diffraction (EBSD) and atomic force microscopy (AFM) to determine texture, microtexture, and grain boundary energies in ceramics, *ICOTOM-12*, 1999.

Green, D.J. (1998) *An Introduction to the Mechanical Properties of Ceramics*, Cambridge University Press, U.K.

Kuszyk, J.A. and Bradt, R. (1973) Influence of grain size on effects of thermal expansion anisotropy in $MgTi_2O_5$, *Journal of the American Ceramic Society*, Vol. 56, No. 8, pp. 420-3.

OOF version 1.0.7 (1999) Center for Theoretical and Computational Materials Science (CTCMS), *National Institute of Standards and Technology (NIST)*, Gaithersburg, MD.

Powell-Dogan, C.A. and Heuer, A.H. (1990) Microstructure of 96% alumina ceramics: III, Crystallization of high-calcia boundary glasses, *Journal of the American Ceramic Society*, Vol. 73, No. 12, pp. 3684-91.

Zimmerman, A., Carter, W.C., and Fuller, E.R. (1999) Damage evolution during microcrack formation in brittle solids, Submitted to *Acta Materialia.*

Sandia is a multiprogram laboratory operated by Sandia Corporation, a Lockheed Martin Company, for the United States Department of Energy under Contract DE-ACO4-94AL85000

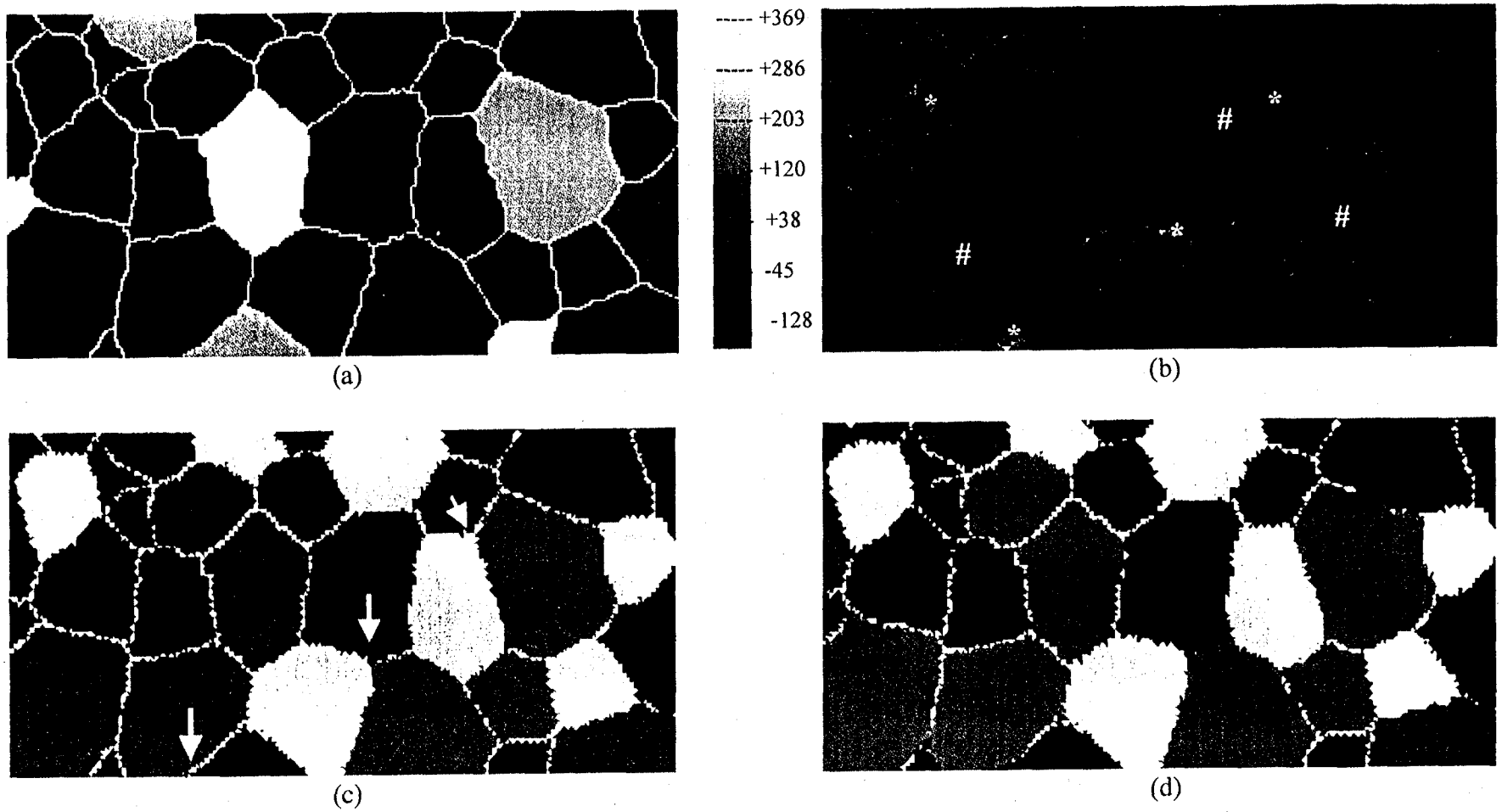

Fig.1: (a) Digital image of alumina (grain size=27μm) (b) Maximum principal stress (σ_{11}) when ΔT=-1160°C, from 369 MPa to −128 MPa (c) crack initiations at ΔT=-1500, shown by black elements along the grain boundaries (d) Damage evolution and distribution at ΔT=-2000°C